

Semiclassical dynamics and long time asymptotics of the central-spin problem in a quantum dot

Gang Chen¹, Doron L. Bergman¹, and Leon Balents¹

¹*Department of Physics, University of California, Santa Barbara, CA 93106-9530*

(Dated: October 17, 2018)

The spin of an electron trapped in a quantum dot is a promising candidate implementation of a qubit for quantum information processing. We study the central spin problem of the effect of the hyperfine interaction between such an electron and a large number of nuclear moments. Using a spin coherent path integral, we show that in this limit the electron spin evolution is well described by classical dynamics of both the nuclear and electron spins. We then introduce approximate yet systematic methods to analyze aspects of the classical dynamics, and discuss the importance of the exact integrability of the central spin Hamiltonian. This is compared with numerical simulation. Finally, we obtain the asymptotic long time decay of the electron spin polarization. We show that this is insensitive to integrability, and determined instead by the transfer of angular momentum to very weakly coupled spins far from the center of the quantum dot. The specific form of the decay is shown to depend sensitively on the form of the electronic wavefunction.

PACS numbers: 73.21.La, 85.35.Be, 72.25.Rb

I. INTRODUCTION

A single electron in a quantum dot provides a versatile experimental realization of a single quantum bit (“qubit”). The electron can be trapped with a high degree of certainty by utilizing the Coulomb blockade effect, in which a large charging energy prevents the motion of electrons on or off the dot. The two level degree of freedom of the qubit is provided then by the electron spin. The electron can be readily manipulated electrically and optically. A limiting factor in such manipulations is “decoherence”, caused by coupling of the electron spin to other degrees of freedom. In high-quality GaAs quantum dots, in which all extrinsic sources of decoherence can be removed, the hyperfine interaction with nuclear moments becomes dominant.^{1,2,3}

In a typical quantum dot, the electron spin is coupled to a very large number $N \sim 10^4 - 10^6$ of nuclear moments, with a range of hyperfine exchange constants determined by the wavefunction of the confined electron. This varies smoothly from near zero at the fringes of the dot to a maximum value near the dot center. To a rather good approximation, there is no direct interaction between different nuclear moments. The latter is present only due to dipolar coupling, but is very small due to the tiny nuclear dipole moment. When it is neglected (which is expected to be a good approximation for a relatively long time $\sim 10^{-3}$ sec), the Hamiltonian \mathcal{H} of the electron-nuclear system has the “central spin” form, in which each nuclear spin operator \vec{I}_i (of spin I) is coupled only to the *central* electron spin ($1/2$) operator \vec{S} :

$$\mathcal{H} = \sum_i a_i \vec{I}_i \cdot \vec{S}. \quad (1)$$

The exchange constants a_i vary with the amplitude of the electron wavefunction in the Quantum dot, at the positions \vec{r}_i of the nuclei: $a_i \sim |\psi(\vec{r}_i)|^2$.

The central spin model is therefore of considerable experimental relevance. It is also of particular theoretical interest. Most intriguingly, it is known that electron spin decoherence within this model is highly non-conventional. For instance, the relaxation of an initially polarized electron spin is *non-exponential*. Indeed, numerical simulations for some specific forms of the electron wavefunction indicated an inverse-logarithmic remanent polarization at long times:^{4,5,6}

$$\langle S^z(t) \rangle \sim \frac{A}{|\ln t|^\alpha}, \quad (2)$$

with the initial condition $S^z(0) = +1/2$ and random unpolarized initial conditions for the nuclear spin state (see Sec. II A); these numerical results suggested $\alpha \approx 1$.

One possible reason to expect unusual behavior in the central spin problem is that it is *integrable*. In fact, the central spin Hamiltonian is a member of a large family of models studied by Gaudin, possessing an infinite number of commuting constants of the motion, both classically and quantum mechanically. The Gaudin models unify the central spin problem with another problem of recent interest, the reduced BCS Hamiltonian for a small disordered superconducting grain. This integrability has attracted additional theoretical attention,^{7,8} but as is often the case, it is quite difficult to extract real-time dynamical properties despite the model’s formal solubility. In any case, it is not clear from these studies whether the unconventional long-time dynamics should be ascribed to integrability or has another origin.

Another controversial aspect of the central spin problem is the significance of *quantum* coherence to the observed behavior. The pioneering studies in Refs. 2,3,9 insist upon a full quantum treatment, but employ approximations valid only in a large applied magnetic field or for nearly full nuclear polarization. The work of Ref.6 instead argued on physical grounds for the validity of the classical approximation, and integrated the classical

equations of motion for the spins numerically, with however no assumptions on the magnetic field or polarization (the focus was largely on the low field and polarization situation most relevant to experiment). Refs.4,5,10 argue for a hybrid approach in which *effective* classical equations of motion are employed using renormalized parameters, finding good agreement with fully quantum simulations on small systems of 15 – 20 spins.

In this paper, we will attempt to clarify the above issues through a combination of techniques. We will first argue, in agreement with Ref.6, that the classical approximation for the nuclear spins is indeed justified *for measurements of the electron spin dynamics* in the physically relevant large N limit. We show this by a simple direct analysis of the exact quantum expression (“Keldysh-like form”) for the time-dependent expectation value of the electron spin, thereby obtaining the explicit connection between the properly defined quantum observable and the classical dynamics. The regime of validity of this approximation is discussed, and open issues highlighted.

Next, having established the correctness of the classical limit, we attack the problem of the anomalous long-time spin dynamics. Despite the simplification of the classical limit, the dynamics remains highly non-linear and non-trivial, and still is not easily accessed using integrability – though some progress has been made in this way for the BCS problem^{7,8,11}. We will argue that the observed long-time behavior is due not to integrability but rather to the effects of very weak but non-zero coupling of the electron to spins far from the center of the dot, in the tails of the electron wavefunction. As time proceeds, successively more weakly coupled nuclear spins are able to influence the electron spin dynamics, leading to a slow change in the latter’s behavior. To address the effects of integrability, we employ a phase space approach inspired by fundamentals of statistical mechanics. In general, one expects (the ergodicity assumption) a Hamiltonian system to equally explore over sufficiently long times all of its phase space accessible by the constraints of its conservation laws. An important feature particular to the central spin problem is the presence of very weakly coupled spins in the tails of the electron wave function. Even for very long times, some such spins have not yet been able to evolve appreciably, further restricting the phase space which has been accessed up to this time. We capture this physics through a crude but effective approximation. For any given time t , we divide the nuclear spins into two groups: those with sufficiently large couplings to the electron spin to allow them to precess through an angle of $O(1)$, and those with weaker couplings that have not. We then neglect completely the latter “decoupled” spins, and treat the former “coupled” spins as an isolated subsystem, and assume that it *has fully explored its accessible phase space already in the time t* . In this “instantaneous ergodicity” approximation, the long time dynamics is due to the continual growth of the ergodic subsystem by inclusion of additional weakly-coupled spins as time progresses.

To study the properties of the ergodic average of the coupled subsystem at any given time, one must still deal with the effects of integrability. Specifically, since the central spin problem is integrable for any number of nuclear spins, the accessible phase space is especially highly constrained due to the infinite number of constants of the motion. We contend, however, that the constraints of integrability are secondary to the already-described physics of weakly coupled spins. The basis of this conclusion is a re-organization of the integrals of motion into an ordered set in which successive integrals manifestly have less influence upon the electron spin. The first four (and therefore most important) integrals of motion in this set are the three components of the total angular momentum and the energy. We find that *ignoring* all remaining integrals of motion, i.e. replacing averages over times less than t by a uniform phase space average in the coupled system at time t *without these constraints*, already reproduces the observed non-exponential long-time spin relaxation. We show how additional integrals of motion can be systematically included in this analysis, and compare the results to numerical simulations.

For the specific forms of wavefunction employed in prior numerical simulations, an inverse logarithmic relaxation is obtained for long times, in agreement with those numerical results. This form is, however, *not* universal, and depends in particular upon the manner in which the electron’s wavefunction approaches zero. The result can be understood rather simply as follows. Because the electron is coupled to many nuclei, its characteristic precession frequency is much larger than the rate at which any of the individual nuclei themselves evolve, as they are coupled only to the single electron spin. Under this condition, as pointed out in Ref. 6, the time-averaged electron spin simply follows the evolution of the net hyperfine field

$$\mathbf{H}_N = \sum_j a_j \mathbf{I}_j. \quad (3)$$

Because the hyperfine couplings a_j decay with the distance of the spin \mathbf{I}_j from the center of the dot, the above hyperfine field can be crudely approximated by including only those N_s spins whose couplings are approximately constant and equal to the maximal a_{\max} :

$$\mathbf{H}_N \approx a_{\max} \sum_{j=1}^{N_s} \mathbf{I}_j. \quad (4)$$

Thus the hyperfine field is approximately proportional to the total angular momentum of these N_s strongest-coupled spins. The total angular momentum of *all* spins is however conserved, and therefore cannot decay but can only be redistributed. Because there is no preference for how this angular momentum is spread amongst the system’s spins, it is natural to expect that over long times, the total angular momentum of all $N(t)$ spins which are appreciably involved in the dynamics is uniformly dis-

tributed amongst them, and we have simply

$$\langle S^z(t) \rangle \sim \langle H_N^z \rangle \sim \frac{N_s}{N(t)}. \quad (5)$$

The time-dependence of $N(t)$ is determined from the fact that, at a large time t , the dynamical spins are those which have had time to precess, i.e. for which $a_j St \gtrsim 1$.

We can in this way readily understand the logarithmic behavior of Eq.(2) for the wavefunctions studied in Refs.6,5. For these Gaussian and exponential wavefunctions,

$$a_j \sim |\psi(\vec{r}_j)|^2 \sim e^{-\left(\frac{r_j}{R_s}\right)^\gamma}, \quad (6)$$

where R_s gives the ‘‘radius’’ of the dot and determines the number of strongly coupled nuclear spins, $N_s \sim R_s^d$, for a d -dimensional dot. The parameter $\gamma = 1, 2$ for exponential and Gaussian wavefunctions, respectively. The dynamical spins at time t are then those inside some radius $R(t)$ such that

$$\frac{R(t)}{R_s} \sim (\ln t)^{1/\gamma}. \quad (7)$$

From Eq.(5), we then obtain Eq.(2) with $\alpha = d/\gamma$. For the two-dimensional quantum dots ($d = 2$) studied in Refs.6,5, this gives $\alpha = 2, 1$ for the exponential and Gaussian wavefunctions, respectively. In Sec.V we obtain these and some other results from the above-described analytic calculations.

The remaining parts of the paper are organized as follows. In Sec. II, we use spin coherent path integral to derive the semi-classical equation of motion for both electron spin and nuclear spins in the large N (number of nuclear spins) limit. In Sec. III, we make a short-time approximation to the classical equations of motion and then focus on the nuclear subsystem. Having systematically argued the relative importance of the integrals of motion, we derive the long time average of effective nuclear field by only considering the most important integrals of motion. The results from the numerical simulation and approximate predictions given in Sec. III are compared in Sec. IV. Finally in Sec. V, with the approximation explained above, the asymptotic time dependence of $\langle S^z(t) \rangle$ is obtained for gaussian, exponentially decaying and hard wall confining boundary coupling profiles. We conclude in Sec.VI with a summary and discussion of future prospects for theoretical development and comparison with experiment.

II. MODEL AND SEMICLASSICAL LIMIT

A. Formulation

We begin by formulating a specific dynamical problem described by the central spin Hamiltonian in Eq.(1).

Specifically, we consider a general initial state in which the electron spin is polarized up:

$$|\Psi(0)\rangle = \sum_{m_1, \dots, m_N} C_{m_1, \dots, m_N} |m_1, \dots, m_N\rangle_I \left| \frac{1}{2} \right\rangle_S, \quad (8)$$

where subindex I, S mean nuclear subsystem and electron, respectively. And $I_i^z = m_i$. The complex coefficients C_{m_1, \dots, m_N} will be taken as independent zero mean Gaussian random variables for each set of m_i . The distribution is then fully specified by the variance

$$\overline{C_{m_1, \dots, m_N}^* C_{m'_1, \dots, m'_N}} = p(m_1, \dots, m_N) \delta_{m_1 m'_1} \dots \delta_{m_N m'_N}, \quad (9)$$

where $p(m_1, \dots, m_N)$ is a normalized ‘‘classical’’ probability distribution for the z-components of the nuclear spins. We will work with the general form

$$p(m_1, \dots, m_N) = \frac{1}{Z} e^{h \sum_i m_i}, \quad (10)$$

where $Z = (\sinh[(I + 1/2)h] / \sinh(h/2))^N$ by normalization. The parameter h specifies the degree of initial nuclear polarization along the $+z$ axis, with $h = 0$ being unpolarized and $h \rightarrow \infty$ for full polarization.

The remanent electron spin polarization is then defined as

$$C(t) \equiv \langle S^z(t) \rangle = \langle \Psi(0) | S^z(t) | \Psi(0) \rangle, \quad (11)$$

where as usual, in the Heisenberg picture,

$$\vec{S}(t) = e^{i\mathcal{H}t} \vec{S} e^{-i\mathcal{H}t}. \quad (12)$$

It has been observed numerically⁵ that $\langle \vec{S}(t) \rangle$ defined in this way is essentially *self-averaging*, i.e independent of the realization of the coefficients in Eq.(8). In Appendix. A, we demonstrate that this is indeed the case for $N \gg 1$, by showing that the normalized fluctuations become *exponentially* small in this limit:

$$\frac{\overline{\langle S^z(t) \rangle^2} - \left(\overline{\langle S^z(t) \rangle} \right)^2}{\left(\overline{\langle S^z(t) \rangle} \right)^2} \lesssim \left(\frac{\tanh(\frac{1}{2}h)}{\tanh[(I + \frac{1}{2})h]} \right)^N, \quad (13)$$

since the quantity in the brackets is always less than unity. Therefore one may approximate

$$C(t) \approx \overline{C(t)} = \overline{\langle S^z(t) \rangle}. \quad (14)$$

The latter averaged quantity is considerably simpler to treat theoretically.

Using Eqs. (8,9,10) one obtains therefore

$$C(t) \approx \frac{1}{Z} \left\langle \frac{1}{2} \right| \text{Tr}_I [e^{-\tilde{\mathcal{H}}/2} e^{i\mathcal{H}t} S^z e^{-i\mathcal{H}t} e^{-\tilde{\mathcal{H}}/2}] \left| \frac{1}{2} \right\rangle_S, \quad (15)$$

with the Boltzmann-like factor

$$\tilde{\mathcal{H}} = -h \sum_i I_i^z. \quad (16)$$

The partial trace and its contents in Eq.(15) are extremely reminiscent of a conventional equilibrium correlation function. The only difference is the presence of the electron spin operator inside the Hamiltonian \mathcal{H} .

To bring out this connection, we introduce a partial Trotter decomposition for the exponentials. We make use of the spin coherent states, with the general form for spin J :

$$|\hat{n}\rangle = \mathcal{R}(\theta, \phi)|J, +J\rangle. \quad (17)$$

Here the $\mathcal{R}(\theta, \phi)$ is the rotation operator that changes the quantization axis from \hat{z} to the direction defined by the angles (θ, ϕ) . The resolution identity in this basis is

$$\frac{2J+1}{4\pi} \int d\hat{n} |\hat{n}\rangle \langle \hat{n}| = 1, \quad (18)$$

where the integration is over the directions on the unit sphere. Similarly the trace is given by

$$\text{Tr}\mathcal{O} = \frac{2J+1}{4\pi} \int d\hat{n} \langle \hat{n} | \mathcal{O} | \hat{n} \rangle. \quad (19)$$

We first use these coherent states *for the electron spin only* to decompose the exponentials of $\pm i\mathcal{H}t$, and obtain the path-integral expressions

$$\begin{aligned} e^{-i\mathcal{H}t} &= \int [d\hat{n}_+(t)] e^{iS_B[\hat{n}_+]} \hat{T}_t^+ e^{-iS \int_0^t dt' \hat{n}_+(t') \cdot \vec{H}} |\hat{n}_+(t)\rangle \langle \hat{n}_+(0)|, \\ e^{+i\mathcal{H}t} &= \int [d\hat{n}_-(t)] e^{-iS_B[\hat{n}_-]} \hat{T}_t^- e^{-iS \int_0^t dt' \hat{n}_-(t') \cdot \vec{H}} |\hat{n}_-(0)\rangle \langle \hat{n}_-(t)|, \\ \vec{H} &= \sum_i a_i \vec{I}_i, \end{aligned} \quad (20)$$

where \hat{T}_t^+ (\hat{T}_t^-) is the time-ordering (anti-time-ordering) operator. Here and in the following, we will use square brackets to denote a functional integration measure. The overlap between coherent states in the Trotterization induces as usual a Berry phase,

$$S_B[\hat{n}] = S \int_0^t dt' \dot{\phi} \cos \theta, \quad (21)$$

where $\hat{n} = (\sin \theta \cos \phi, \sin \theta \sin \phi, \cos \theta)$ and $S = 1/2$. Because the different nuclear spin operators in each term of the sum defining \vec{H} (Eq.(20)) commute, the operator exponentials can be factored. Using then Eq.(20) in Eq.(15), and expressing the trace over the nuclear subspaces using Eq.(19), one obtains

$$\begin{aligned} C(t) &= \frac{1}{Z} \int \prod_i d\hat{n}_i \int [d\hat{n}_+ d\hat{n}_-] \\ &e^{i(S_B[\hat{n}_+] - S_B[\hat{n}_-])} \langle \hat{n}_-(t) | S^z | \hat{n}_+(t) \rangle \\ &\prod_i \langle \hat{n}_i | e^{hI_i^z/2} U_i^-(0, t) U_i^+(0, t) e^{hI_i^z/2} | \hat{n}_i \rangle, \end{aligned} \quad (22)$$

where $\tilde{Z} = Z(4\pi/(2I+1))^N$, $|\hat{n}_i\rangle$ is a coherent state for the nuclear spin \vec{I}_i , and

$$U_i^\pm(t_1, t_2) = T_t^\pm e^{\mp i a_i S \int_{t_1}^{t_2} dt \hat{n}_\pm(t) \cdot \vec{I}_i}. \quad (23)$$

Inspecting Eq.(22), we note that the integrand of the functional integrals over $\hat{n}_\pm(t)$ contains a product of N factors – expectation values in the state $|\hat{n}_i\rangle$ – one for each individual nuclear subspace. Each such factor is a *functional* of $\hat{n}_\pm(t)$, and is distinguished from the others *only* by its value of a_i (and the state \hat{n}_i). Since there are many ($O(N)$) such factors all with a_i of the same order, this product is sharply-peaked/rapidly-oscillating and renders the path integral suitable for a saddle point expansion (formally it can be rewritten in the usual form as the exponential of a sum of N smoothly-varying terms). We will see below that the Berry phase terms are also rapidly oscillating.

The saddle point equations are:

$$\begin{aligned} \frac{\delta}{\delta \hat{n}_\pm(t')} \left[\sum_i \ln \langle \hat{n}_i | e^{hI_i^z/2} U_i^-(0, t) U_i^+(0, t) e^{hI_i^z/2} | \hat{n}_i \rangle \right. \\ \left. \pm i S_B[\hat{n}_\pm] \right] = 0. \end{aligned} \quad (24)$$

This saddle point equation actually leads to the classical equations of motion. To see this, we evaluate the functional derivatives in Eq.(24). The variation of the Berry phase term is well known¹²:

$$\frac{\delta S_B}{\delta \hat{n}_\pm} = S \hat{n}_\pm \times \dot{\hat{n}}_\pm. \quad (25)$$

The variation of the expectation value is more involved:

$$\begin{aligned} \frac{\delta}{\delta \hat{n}_\pm(t')} \ln \langle \hat{n}_i | e^{hI_i^z/2} U_i^-(0, t) U_i^+(0, t) e^{hI_i^z/2} | \hat{n}_i \rangle \\ = \mp i a_i S \langle \vec{I}_i \rangle_{t't'}^\pm, \\ \langle \vec{I}_i \rangle_{t't'}^+ = \frac{\langle \hat{n}_i | e^{hI_i^z/2} U_i^-(0, t) U_i^+(t', t) \vec{I}_i U_i^+(0, t') e^{hI_i^z/2} | \hat{n}_i \rangle}{\langle \hat{n}_i | e^{hI_i^z/2} U_i^-(0, t) U_i^+(0, t) e^{hI_i^z/2} | \hat{n}_i \rangle} \\ \langle \vec{I}_i \rangle_{t't'}^- = \frac{\langle \hat{n}_i | e^{hI_i^z/2} U_i^-(0, t) \vec{I}_i U_i^-(t', t) U_i^+(0, t') e^{hI_i^z/2} | \hat{n}_i \rangle}{\langle \hat{n}_i | e^{hI_i^z/2} U_i^-(0, t) U_i^+(0, t) e^{hI_i^z/2} | \hat{n}_i \rangle}. \end{aligned} \quad (26)$$

Thus the saddle point equations become:

$$\hat{n}_\pm(t') \times \dot{\hat{n}}_\pm(t') = \sum_i a_i \langle \vec{I}_i \rangle_{t't'}^\pm. \quad (27)$$

These equations are solved by the restricted condition $\hat{n}_+(t') = \hat{n}_-(t') \equiv \hat{n}(t')$. We then accordingly write $U_i^+(t_1, t_2) \equiv U_i(t_1, t_2)$ and one has $U_i^-(t_1, t_2) = [U_i(t_1, t_2)]^\dagger$. One obtains

$$\langle \vec{I}_i \rangle_{t't'}^\pm = \frac{\langle \hat{n}_i | e^{hI_i^z/2} [U_i(0, t')]^\dagger \vec{I}_i U_i(0, t') e^{hI_i^z/2} | \hat{n}_i \rangle}{\langle \hat{n}_i | e^{hI_i^z} | \hat{n}_i \rangle} \equiv \mathbf{I}_i(t'). \quad (28)$$

The ‘‘classical’’ nuclear spin variable defined in this way has the form of the expectation value of a standard Heisenberg operator. Thus it obeys

$$\partial_t \mathbf{I}_i = a_i \mathbf{S} \times \mathbf{I}_i, \quad (29)$$

with

$$\mathbf{S} = S \hat{n}, \quad (30)$$

and the initial condition

$$\begin{aligned} I_i^{x,y}(t=0) &= I \frac{n_i^{x,y}}{\cosh(h/2) + \sinh(h/2)n_i^z}, \\ I_i^z(t=0) &= I \frac{\cosh(h/2)n_i^z + \sinh(h/2)}{\cosh(h/2) + \sinh(h/2)n_i^z}, \end{aligned} \quad (31)$$

and $I_i^z(0) = I^2$, in the unpolarized case when $h = 0$, the above expression reduces to a simple form $\mathbf{I}_i(0) = I \hat{n}_i$. Combining the results of Eqs.(27),(28) and the definition in Eq.(30), the saddle point equation itself reduces to

$$\partial_t \mathbf{S} = \mathbf{H}_N \times \mathbf{S}, \quad (32)$$

$$\mathbf{H}_N = \sum_i a_i \mathbf{I}_i. \quad (33)$$

Because of the polarized initial electron spin state, one has

$$\mathbf{S}(t=0) = S \hat{z}. \quad (34)$$

Note that Eqs. (29,31,32,34) are precisely the classical equations of motion for this system, with the specified initial conditions. The remanent polarization is obtained from these classical variables by evaluating the path integrals over $\hat{n}_\pm(t')$ at the saddle point, and performing the remaining integrations over the \hat{n}_i variables:

$$C(t) = [S^z(t; \{\hat{n}_i\})]. \quad (35)$$

Here $S^z(t; \{\hat{n}_i\})$ is the solution to the classical equations of motion for the nuclear initial conditions specified in Eq.(31), evaluated at time t , and the square brackets indicate an average over the nuclear initial conditions:

$$[A(\{\hat{n}_i\})] = \frac{\int \prod_i d\hat{n}_i [\cosh(h/2) + \sinh(h/2)n_i^z]^{2I} A(\{\hat{n}_i\})}{\int \prod_i d\hat{n}_i [\cosh(h/2) + \sinh(h/2)n_i^z]^{2I}}. \quad (36)$$

The normalization is determined by the requirement that $C(0) = 1/2$.

III. CLASSICAL ANALYSIS

A. Reduced nuclear equations

In the previous section we showed the classical equations of motion are a good approximation for the dynamics of the system. In this section we proceed to analyze them. The classical equations of motion read

$$\begin{aligned} \partial_t \mathbf{S} &= \mathbf{H}_N \times \mathbf{S} \\ \partial_t \mathbf{I}_j &= a_j \mathbf{S} \times \mathbf{I}_j, \end{aligned} \quad (37)$$

where $\mathbf{H}_N = \sum_j a_j \mathbf{I}_j$ acts as an effective magnetic field, which the electron spin precesses about. Here $|\mathbf{S}| = S = 1/2$ and $|\mathbf{I}_j| = I$.

Since the magnitude of the effective field $\mathbf{H}_N \equiv |\mathbf{H}_N|$ is of order $\sim \sqrt{N}$, while an individual nuclear spin couples with only the single electron spin, the timescale of the dynamics for the nuclear spins is much longer than the electron spin.¹³ As a result, electron spin precesses rapidly about an axis which itself moves only much more slowly with time:

$$\mathbf{S}(t) = \langle \mathbf{S} \rangle_t + \sqrt{S^2 - |\langle \mathbf{S} \rangle_t|^2} \text{Re}[(\mathbf{e}_1 + i\mathbf{e}_2)e^{i\mathbf{H}_N t}], \quad (38)$$

where $\mathbf{e}_1, \mathbf{e}_2$ are orthogonal unit vectors in the plane perpendicular to the short-time average of the electron spin $\langle \mathbf{S} \rangle_t$,

$$\langle \mathbf{S} \rangle_t = S \cos \theta_0 \hat{\mathbf{m}}, \quad (39)$$

which itself is along the axis $\hat{\mathbf{m}}$ of the effective nuclear field

$$\hat{\mathbf{m}} = \frac{\mathbf{H}_N}{H_N}. \quad (40)$$

The vectors $\hat{\mathbf{m}}, \mathbf{e}_1, \mathbf{e}_2$ form an orthonormal frame, and vary on timescales much slower than the electron precession quasi-period $1/H_N$. The parameter θ_0 is the initial angle between the electron spin polarization and $\mathbf{H}_N(t=0)$. To study the dynamics of the nuclear spin, it is sufficient (for large N) to replace the electron spin by its time average, leading to reduced equations of motion

$$\partial_t \mathbf{I}_j = g_j \hat{\mathbf{m}} \times \mathbf{I}_j, \quad (41)$$

With $g_j = S \cos \theta_0 a_j$. Eqs.(41) eliminate the electron spin completely, and form a closed description of the nuclear dynamics. They are equivalent to the Hamiltonian

$$\mathcal{H}_{\text{eff}} = S \cos(\theta_0) H_N, \quad (42)$$

which involves only the nuclear spins.

B. Conserved quantities

From the Hamiltonian in Eq.(41), it is obvious the magnitude of the effective field H_N is a *conserved* quantity. By spin-rotational invariance, the total spin angular momentum is conserved, which in the above time-averaged electron approximation becomes conservation of just the total nuclear spin $\mathbf{I} = \sum_i \mathbf{I}_i$ (the electron’s contribution to the total spin of the system is negligible for large N). It is readily verified that \mathbf{I} is indeed conserved directly from Eq.(41).

In fact one can find a series of conserved quantities for the reduced equations of motion, obtained in the same way from those for the complete central spin problem¹¹

$$\mathcal{H}_q = \sum_{j \neq q} \frac{2g_j g_q}{g_j - g_q} \mathbf{I}_q \cdot \mathbf{I}_j, \quad (43)$$

where $q = 1, \dots, N$ runs over all the nuclear spins, and we have assumed that no two nuclear spins have the same coupling g_j to the electron spin (this is a simplifying but inessential assumption for our purposes).

It will be convenient to consider a different linear combination of these constants of the motion, which are naturally also conserved:

$$\mathcal{C}_n = \sum_q g_q^n \mathcal{H}_q. \quad (44)$$

The \mathcal{C}_n can be defined for any n , and any set containing N members of \mathcal{C}_n 's is completely equivalent to the original set of $\{\mathcal{H}_q\}$, because the matrix determinant of this linear transformation from $\{\mathcal{H}_q\}$ to $\{\mathcal{C}_n\}$ is nonvanishing, as all the couplings are different. Also notice that the original set of \mathcal{H}_q is linearly independent *except* for one constraint

$$\mathcal{C}_0 = \sum_{q=1}^n \mathcal{H}_q = 0, \quad (45)$$

which follows from Eq.(43). The energy $S \cos(\theta_0) \mathbf{H}_N$ and magnitude of the total spin are contained in this set via

$$\mathcal{C}_1 = -S^2 \cos^2(\theta_0) \mathbf{H}_N^2 + I^2 \sum_j g_j^2, \quad (46)$$

$$\mathcal{C}_{-1} = I^2 - I^2 N, \quad (47)$$

where $I = \|\mathbf{l}\|$.

C. Collective variables and steady-state relations

It is useful to define a set of vector quantities, which serve as collective variables:

$$\mathbf{h}_n \equiv \sum_j g_j^n \mathbf{I}_j. \quad (48)$$

And $\mathbf{h}_1 = S \cos(\theta_0) \mathbf{H}_N$, $\mathbf{h}_0 = \mathbf{l}$. The values of \mathbf{h}_n determine the constants of motion \mathcal{C}_n (but not vice-versa):

$$n > 0, \quad \mathcal{C}_n = - \sum_{k=1}^n \mathbf{h}_k \cdot \mathbf{h}_{n+1-k} + n I^2 \sum_j g_j^{n+1} \quad (49)$$

$$n < 0, \quad \mathcal{C}_n = \sum_{k=0}^{-n-1} \mathbf{h}_{-k} \cdot \mathbf{h}_{n+1+k} + n I^2 \sum_j g_j^{n+1} \quad (50)$$

In addition, the \mathbf{h}_n 's obey simple dynamical equations obtained by taking moments of the equations of motion, Eq.(41):

$$\partial_t \mathbf{h}_n = \hat{\mathbf{m}} \times \mathbf{h}_{n+1}. \quad (51)$$

Here, we have expressed the spin dynamics completely in terms of these collective variables. Any set of N contiguous collective variables, $\{\mathbf{h}_k, \dots, \mathbf{h}_{k+N-1}\}$ for any k , is equivalent to the original spin variables. This is because Eq.(48) defines a linear transformation of the van

der Monde form, whose determinant is therefore non-vanishing provided none of the g_j are equal, as assumed. Furthermore, the field \mathbf{h}_{k+N} appearing in the equation of motion (Eq.(51)) for $\partial_t \mathbf{h}_{k+N-1}$ can be eliminated in favor of this set since it is not linearly independent of them, leading to closed equations of motion for the collective variables.

The point of view in which the \mathbf{h}_n are taken as our dynamical variables is useful for elucidating the relative importance of the \mathcal{C}_n for positive n . The constants of motion of course prevent the collective variables from ergodically exploring all of phase space. We are interested primarily in the nuclear hyperfine field \mathbf{h}_1 . From Eq.(49), clearly all \mathcal{C}_n for $n > 0$ involve \mathbf{h}_1 , and thereby restrict somewhat its evolution. However, the invariants for increasing n involve progressively more terms which *do not* include \mathbf{h}_1 . Thus we expect the corresponding constraints to be less restrictive on the average nuclear field.

Conversely, to understand the (in)significance of invariants \mathcal{C}_n with *negative* n is more readily seen in the original nuclear spin variables. Specifically, when $n < 0$, greater weight is given in \mathcal{C}_n to those nuclear spins with the *weakest* couplings to the electron (and hence to each other in the effective equation of motion). Therefore we expect these integrals of motion to play successively weaker roles in the dynamics in general, and especially in the dynamics of the electron. Consequently, we focus on the \mathcal{C}_n with small positive n .

Suppose we consider the infinite time limit for a finite system $N < \infty$. Let us consider the time average of some physical quantity over this time, defined by

$$\langle \mathcal{O} \rangle \equiv \lim_{\tau \rightarrow \infty} \frac{1}{\tau} \int_0^\tau dt \mathcal{O}(t). \quad (52)$$

In ergodic systems, this limit is well-defined for most quantities. In integrable systems, the existence of this limit may depend upon which quantity is averaged. Consider the time average of Eq.(51) for $n = -1$. Since $\mathbf{h}_0 = \mathbf{l}$, it is conserved and thus time-independent, and can be brought outside the time average. Therefore, one has

$$\langle \partial_t \mathbf{h}_{-1} \rangle = -\mathbf{l} \times \langle \hat{\mathbf{m}} \rangle. \quad (53)$$

If we now assume both $\langle \hat{\mathbf{m}} \rangle$ and $\langle \mathbf{h}_{-1} \rangle$ are well-defined, then the left-hand-side in Eq.(53) *vanishes*. Thus we conclude $\mathbf{l} \times \langle \hat{\mathbf{m}} \rangle = 0$, i.e. the time average of the nuclear field is parallel to the total angular momentum:

$$\langle \hat{\mathbf{m}} \rangle = \kappa \frac{\mathbf{l}}{I}. \quad (54)$$

The proportionality constant must satisfy $|\kappa| \leq 1$ since $\hat{\mathbf{m}}$ is a unit vector. If $|\kappa| \neq 1$, this indicates persistent motion of the nuclear field in the asymptotic time evolution. Our numerics actually show that κ is a convergent quantity.

D. Approximate treatment of time averages

Despite the very large number of integrals of motion, a complete analytic solution of this problem has eluded the community. In this section, we adopt a less ambitious but more pragmatic approach, and attempt to calculate the long-time average of the nuclear field asymptotically. We do this by first making the quasi-ergodic assumption that this time average is equivalent to a uniform average over the accessible regions of phase space. The latter average is analogous to a microcanonical ensemble average in statistical mechanics, but with more constraints provided not only by energy conservation but by the many integrals of motion. Mathematically, using the integrals \mathcal{C}_n , one has

$$\langle \hat{\mathbf{m}} \rangle_p = \frac{1}{\mathcal{Z}_p} \int \mathcal{D}[\mathbf{I}_j] \hat{\mathbf{m}} \delta\left(\sum_j \mathbf{I}_j - \mathbf{l}\right) \delta\left(\left|\sum_j a_j \mathbf{I}_j\right| - H_N\right) \times \prod_{n=2}^p \delta(\mathcal{C}_n - c_n), \quad (55)$$

where c_n are the fixed values of the integrals \mathcal{C}_n , $\mathcal{D}[\mathbf{I}_j] = \prod_j d\mathbf{I}_j$, and we have introduced the partition function

$$\mathcal{Z}_p = \int \mathcal{D}[\mathbf{I}_j] \delta\left(\sum_j \mathbf{I}_j - \mathbf{l}\right) \delta\left(\left|\sum_j a_j \mathbf{I}_j\right| - H_N\right) \times \prod_{n=2}^p \delta(\mathcal{C}_n - c_n) \quad (56)$$

In addition to this quasi-ergodic assumption, we make a separate approximation, which consists of truncating the $O(N)$ series of constraints in Eqs.((55),(56)) to only the first few. The degree of approximation is determined by the parameter p above. For $p = 1$, we include only energy and angular momentum conservation, while $p > 1$ counts the number of additional conserved quantities taken into account. This approximation is motivated by the fact that, as argued above, the \mathcal{C}_n are expected to have increasingly little influence on the system's dynamics for increasing positive n and negative n .

To calculate $\langle \hat{\mathbf{m}} \rangle_p$ for small p , it is convenient to introduce the (unnormalized) distribution of the vector $\hat{\mathbf{m}}$:

$$P_p(\hat{\mathbf{m}}; \mathbf{l}, H_N) = \int \mathcal{D}[\mathbf{I}_j] \delta\left(\sum_j \mathbf{I}_j - \mathbf{l}\right) \times \delta\left(\sum_j a_j \mathbf{I}_j - H_N \hat{\mathbf{m}}\right) \prod_{n=2}^p \delta(\mathcal{C}_n - c_n). \quad (57)$$

By rotational invariance, this distribution is actually a function only of the angle θ between $\hat{\mathbf{m}}$ and \mathbf{l} and not the absolute directions of either vector. Thus we may write

$$P_p(\hat{\mathbf{m}}; \mathbf{l}, H_N) = P_p(\cos \theta; \mathbf{l}, H_N), \quad (58)$$

with $\hat{\mathbf{m}} \cdot \hat{\mathbf{l}} = \cos \theta \equiv u$. The desired expectation value is then obtained by a simple spherical average as

$$\langle \hat{\mathbf{m}} \rangle_p = \frac{\int_{-1}^1 du u P_p(u) \hat{\mathbf{l}}}{\int_{-1}^1 du P_p(u)}, \quad (59)$$

where we have suppressed the dependence on \mathbf{l}, h_1 .

The distribution $P_p(\cos \theta)$ can be calculated for small p by a saddle point technique (for $N \gg 1$). Details are given in Appendix B. For $p = 1$, one obtains the very simple distribution

$$P_1(\cos(\theta)) = e^{\alpha \cos(\theta)}, \quad (60)$$

with

$$\alpha = \frac{3\bar{a}}{a^2 - \bar{a}^2} \frac{H_N \mathbf{l}}{N I^2}, \quad (61)$$

and we define the moments of exchange couplings

$$\bar{a}^n = \frac{1}{N} \sum_{j=1}^N a_j^n. \quad (62)$$

The resulting average direction from Eq.(59) is then

$$\langle \hat{\mathbf{m}} \rangle_1 = \hat{\mathbf{l}} \left(\coth \alpha - \frac{1}{\alpha} \right). \quad (63)$$

For $\alpha \ll 1$, $\langle \hat{\mathbf{m}} \rangle_1$ has an even simpler expression:

$$\langle \hat{\mathbf{m}} \rangle_1 = \hat{\mathbf{l}} \frac{\alpha}{3} \quad (64)$$

The first improvement upon the above result is to include one additional conserved quantity, which gives (see Appendix B)

$$P_2(\cos \theta) = e^{\gamma \cos \theta + \beta \cos^2 \theta}, \quad (65)$$

where

$$\gamma = \frac{6\mathbf{H}_N^2 (\bar{a}^2 \cdot \bar{a}^3 - \bar{a} \bar{a}^4) + \frac{3IK}{(S \cos \theta_0)^3} (\bar{a} \bar{a}^3 - (\bar{a}^2)^2)}{2N H_N I^2 [(\bar{a}^2)^3 - 2\bar{a}^2 \bar{a} \bar{a}^3 + (\bar{a}^3)^2 - (\bar{a}^2 - (\bar{a})^2) \bar{a}^4]} \\ \beta = \frac{3I^2 (\bar{a} \bar{a}^3 - (\bar{a}^2)^2) / [I^2 (\bar{a}^2 - \bar{a}^2)]}{2N [(\bar{a}^2)^3 - 2\bar{a}^2 \bar{a} \bar{a}^3 + (\bar{a}^3)^2 - (\bar{a}^2 - (\bar{a})^2) \bar{a}^4]}, \quad (66)$$

with $K \equiv 2\mathbf{h}_2 \cdot \mathbf{h}_1 = -\mathcal{C}_2 + 2I^2 \sum_j g_j^3$. The resulting average of the nuclear field direction becomes

$$\langle \hat{\mathbf{m}} \rangle_2 = \hat{\mathbf{l}} \left[\frac{2e^{\frac{\gamma^2}{2\beta} + \beta} \sinh(\gamma)}{\sqrt{\pi} \sqrt{\beta} \left[F\left(\frac{\gamma+2\beta}{2\sqrt{\beta}}\right) - F\left(\frac{\gamma-2\beta}{2\sqrt{\beta}}\right) \right]} - \frac{\gamma}{2\beta} \right], \quad (67)$$

where $F(z)$ is the imaginary error function defined by $F(0) = 0$ and $F'(z) = \frac{2}{\sqrt{\pi}} e^{z^2}$.

In principle, we can take into account more and more conserved quantities. However, the calculation becomes more and more cumbersome.

In the next section, we compare the predictions of this approximate calculation with numerical simulation of the classical equations of motion.

IV. NUMERICAL SIMULATION

In this section we briefly review the numerical simulation of the classical equations of motion for the nuclear spins alone. The equation we are using is Eq.(41). We use a finite difference discretization of the equations of motion to advance the nuclear spins from the initial conditions to any subsequent time.

In order to protect the unit magnitude of the nuclear spins in the finite difference equations, we use a rotation matrix about the effective field \mathbf{H}_N to advance the nuclear spin states from $\{\mathbf{I}_i(t)\}$ to $\{\mathbf{I}_i(t + \Delta t)\}$. Rather than simply advance to the next time step, we use the Euler method - we take the values of $\mathbf{I}_i(t + \Delta t)$, calculate $\frac{1}{2}(\mathbf{H}_N(t) + \mathbf{H}_N(t + \Delta t))$, and use this new averaged effective field value to produce new values for $\mathbf{I}_i(t + \Delta t)$. This procedure is repeated a number of times until $\mathbf{I}_i(t + \Delta t)$ is converged. Mathematically, this above process can be expressed compactly as follows, start with

$$\{\mathbf{I}_i(t)\} \text{ and } \mathbf{H}_N^0(t) = \sum_i a_i \mathbf{I}_i(t),$$

then repeat

$$\begin{aligned} \mathbf{I}_i^k(t + \Delta t) &= \mathcal{R}(\hat{\mathbf{H}}_N^k(t), g_i \Delta t) \mathbf{I}_i(t), \\ \mathbf{H}_N^k(t + \Delta t) &= \sum_i a_i \mathbf{I}_i^k(t + \Delta t), \\ \mathbf{H}_N^{k+1}(t) &= \frac{1}{2}(\mathbf{H}_N^0(t) + \mathbf{H}_N^k(t + \Delta t)), \end{aligned} \quad (68)$$

until

$$|\mathbf{I}_i^{k+1}(t + \Delta t) - \mathbf{I}_i^k(t + \Delta t)| < \epsilon,$$

where, the operation $\mathcal{R}(\hat{\mathbf{m}}, \phi)$ is the rotation about direction $\hat{\mathbf{m}}$ by angle ϕ , the integer variable k is the times repeated, and ϵ is used to measure the convergence.

To verify correctness, we checked for conservation of energy and total angular momentum \mathbf{I} for all the data series we generated. In our simulations we found that these are conserved at an accuracy of $\Delta E/E, |\Delta \mathbf{I}|/I \sim 0.1\% - 0.2\%$. Numerical simulation for a number of special solvable cases were also carried out (“solvable” means they can be solved analytically after the short-time average for electron spin introduced in Sec. III A). These consist of the problem of two nuclear spins with different coupling constants and the problem of many nuclear spins with identical coupling constants. In both cases, we find agreement between the simulations and the analytic results within the numerical accuracy.

We compare using the Euler method with a rotation matrix to the standard finite difference 4th order Runge Kutta in our simulation by finding the distribution $P(\cos \theta)$ (introduced in Sec.III D, and measured by finding the histogram of the variable $\cos \theta$). The two simulations were performed over 500,000 timesteps of 0.05, starting from the same initial conditions for 128 nuclear spins with coupling constants uniformly distributed from

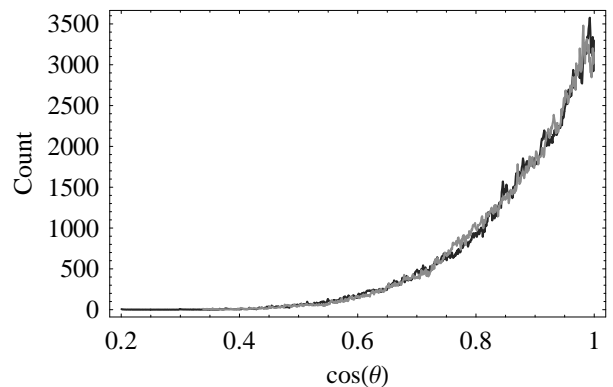


FIG. 1: Comparison between histogram profiles generated by 4th order Runge Kutta and our modified Euler method. The dark gray profile is from data by 4th order Runge Kutta, the light gray one is from our modified Euler method. As expected, they almost coincide with each other.

0 to 1, The two measured distributions agree well, as plotted in Fig.1, but the 4th order Runge Kutta method requires much finer time discretization (smaller Δt) than our modified Euler method in order to preserve energy and total angular momentum to the same degree of accuracy. Furthermore, our modified Euler method more naturally conserves the magnitude of each individual spin vector.

In the simulation we find the complete time evolution of the variable $\cos \theta$. We also find the value of κ defined in Eq.(54). The simulations are carried out for 600,000 timesteps of $\Delta t = 0.1$, with different initial conditions and three different coupling profiles. The approximate theoretical κ values from Eq.(63) and Eq.(67) are plotted against the numerical κ values in Fig.2,3,4 for the different coupling profiles. For each figure, the correlations between numerical data and two theoretical predictions are explicitly calculated and listed in Table. I. For two data sets X and Y , the correlation $\rho_{X,Y}$ between them is defined as

$$\rho_{X,Y} = \frac{\text{cov}(X,Y)}{\sigma_X \sigma_Y}, \quad (69)$$

where $\text{cov}(X,Y)$ is the covariance between X and Y and σ_X, σ_Y are the standard deviation of data set X and Y , respectively. The correlation is 1 in the case of an increasing linear relationship, -1 in the case of a decreasing linear relationship, and some value in between in all other cases, indicating the degree of linear dependence between the variables. The closer the coefficient is to either -1 or 1, the stronger the correlation between the variables. Although for some (very few) initial configurations, the analytical prediction given by Eq.(67) deviates from the numerical values more than Eq.(63), the correlations in the table clearly indicate that analytical prediction by Eq.(67) is much better than Eq.(63). In addition, Eq.(63) always gives positive κ , Eq.(67) can give negative κ as

κ data set	numerics and Eq.(63)	numerics and Eq.(67)
Fig.2	0.817407	0.891817
Fig.3	0.771773	0.926312
Fig.4	0.704288	0.991488

TABLE I: Correlation between κ value data from numerics and two theoretical predictions given by Eq.(63) and Eq.(67) for three different coupling profiles, the data are the same as the ones used in the corresponding figures of the left column above.

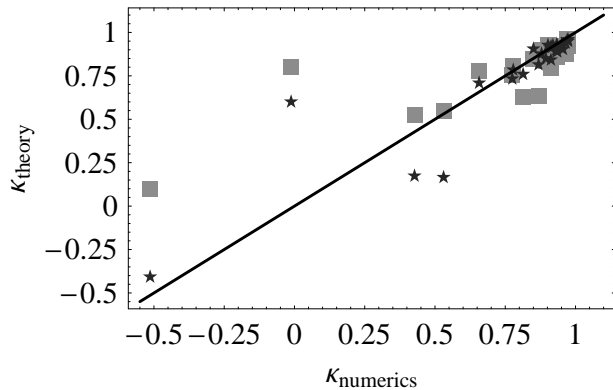


FIG. 2: Comparison of theory and numerics for values of κ . The couplings are given by gaussian coupling profile $a_{i,j} = 2.0 \exp[-\frac{\pi(i^2+j^2)}{400}]$, where i, j are integer values constrained by $i^2 + j^2 \leq 900/\pi$, 900 nuclear spins total. The coordinate of each box(gray) is $(\kappa$ -numerics, κ -Eq.(63)); while the star(black) is $(\kappa$ -numerics, κ -Eq.(67)), same numerical value represents same initial condition. The error bar of the numerical κ is too small to be seen in this figure. In this figure, 39 different initial configurations are generated. The solid line is used as reference line, meaning the exact agreement between theory and numerics. (The same conventions hold for Fig. 3,4)

shown by several points in Fig. 2,4, when the averaged effective nuclear magnetic field is anti-parallel with the total nuclear angular momentum l . The correlation table also indicates that, (though we need more numerics to confirm this indication) Eq.(63) works better for the coupling profiles which are relatively more peaked, Eq.(63) and Eq.(67) works better for the coupling profiles which are more extended. Our explanation for this feature is that, the more peaked the coupling profile is, the better the approximation given by Eq.(4) is; and under this approximation, the collective variables \mathbf{h}_n defined by (48) can be considered roughly proportional to \mathbf{H}_N , so Eq.(63) is probably enough to give relatively good prediction, and Eq.(67) won't improve the prediction significantly as for the more extended coupling profiles.

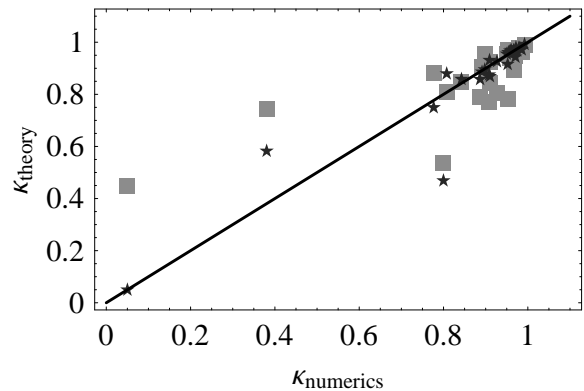


FIG. 3: Comparison of theory and numerics for values of κ . The couplings are given by gaussian coupling profile $a_{i,j} = 2.0 \exp[-\sqrt{\frac{\pi(i^2+j^2)}{400}}]$, where i, j are integer values constrained by $i^2 + j^2 \leq 900/\pi$, 900 nuclear spins total. In this figure, 30 different initial configurations are generated.

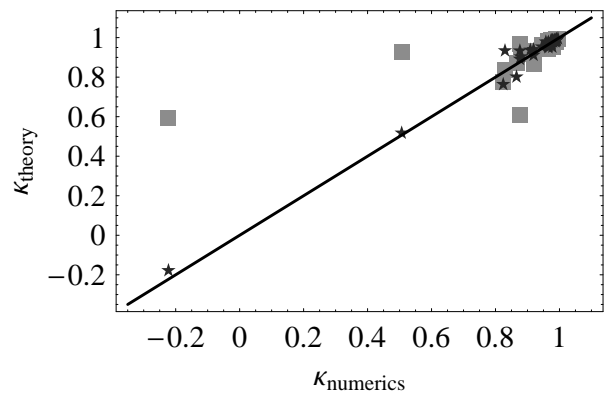


FIG. 4: Comparison of theory and numerics for values of κ . The couplings are given by gaussian coupling profile $a_{i,j} = 2.0 \exp[-\frac{\pi(i^2+j^2)}{1000}]$, where i, j are integer values constrained by $i^2 + j^2 \leq 900/\pi$, 900 nuclear spins total. In this figure, 29 different initial configurations are generated.

V. ASYMPTOTIC BEHAVIOR OF $\langle S^z(t) \rangle$

As discussed in the Introduction, even at long times t there will be some very weakly coupled spins which have not evolved appreciably. These spins, being very weakly coupled to the electron, also do not significantly contribute to its average or to the nuclear hyperfine field. Thus we need consider only the dynamics of those spins with couplings $a_i t \geq k$ with some constant k of $O(1)$. We will keep k as a free parameter in the considerations below to assess the sensitivity of our results to this choice. Quantities which are sensitive to $O(1)$ changes of k are clearly not reliably obtained from our approximations.

Let us for the time being focus on wavefunctions with the (stretched) exponential form of Eq.(6), for which the size of the region of dynamically coupled spins evolves

logarithmically, as given in Eq.(7). For such logarithmic growth, the number of dynamical spins increases extremely slowly at long times, with very few additional spins being added with each proportional increase (e.g. doubling) in time. Thus we believe that the most of the spins within this region have to a very good approximation explored their accessible phase space – subject of course to the constraints of integrability. This is the physical argument justifying the use of Eq.(55) with the time-dependence only appearing through the slow increase of the set of dynamical couplings.

In Sec. III C, we argued that invariants \mathcal{C}_n have decreasing relevance to the electron dynamics with increasing positive n . In the more specialized context of this section, we can slightly refine this contention. Specifically, consider the average $\langle \hat{\mathbf{m}}_p \rangle$ defined in Eq.(55) in the long-time limit. We are interested only in the time-dependence of this quantity, i.e. how it changes as additional very weakly coupled spins \mathbf{I}_j are introduced into the average. These appear in the integration measure, inside the definition of $\hat{\mathbf{m}}$, and in the δ -function constraints due to the constants of the motion. However, in all these places *except* the measure and the δ -function constraining the total angular momentum \mathbf{I} – and specifically in all higher invariants \mathcal{C}_n with $n \geq 2$ – the additional introduced spins are weighted by positive powers of their very small couplings a_j . Thus we expect that all these approximations give very similar long-time dependence for $p \geq 1$. Indeed, by explicit computation (using e.g. Eq.(65) and its generalizations) we found identical results for the leading asymptotic long-time behavior for $p = 1, 2$.

We therefore discuss the simplest but sufficient case $p = 1$, in which only energy and total angular momentum conservation are taken into account. To use Eq.(63) we require α from Eq.(61), which depends upon the first two moments of the hyperfine couplings. Consider the case of a Gaussian wavefunction, $\gamma = 2$ in Eq.(6). Including those nuclear spins at radii $r < R(t)$, one obtains $\bar{a} = \frac{a_0}{\ln(t/k)}$ and $\bar{a}^2 = \frac{a_0^2}{2 \ln(t/k)}$, where a_0 gives the overall scale of the hyperfine coupling. A typical (root mean square ensemble average) value of the combination $\frac{H_N \mathbf{I}}{N I^2} \sim \sqrt{\bar{a}^2} \sim \frac{1}{\sqrt{\ln(t/k)}}$, and for this reason the parameter α

$$\alpha \sim \sqrt{\frac{1}{\ln(t/k)}} \ll 1. \quad (70)$$

Assuming $S^z(0) = 1/2$, then $\cos \theta_0 = \frac{H_N^z}{H_N}$ and we can evaluate the appropriate ensemble average derived in Eq.(35), replacing the classical spin by its short-time av-

erage and using Eq.(39),(64):

$$\begin{aligned} C(t) = \langle S^z(t) \rangle &= \left[\frac{1}{2} \frac{H_N^z(t)}{H_N(t)} \frac{|^z(t)| \alpha}{\mathbf{I}(t)} \frac{\alpha}{3} \right] \\ &= \left[\frac{1}{2} \frac{\bar{a}}{a^2 - \bar{a}^2} \frac{H_N^z(t) |^z(t)}{N I^2} \right] \\ &= \frac{1}{6} \frac{\bar{a}^2}{a^2 - \bar{a}^2} \\ &= \frac{1}{6} \frac{1}{\ln \frac{t}{k}}, \end{aligned} \quad (71)$$

where we have replaced H_N^z/H_N with the effective $H_N^z(t)/H_N(t)$ found within $R(t)$ in the first line of the above equations, as they are very close in the asymptotic time limit, and in the fourth line, the ensemble averaging is taken, where $[H_N^z(t) |^z(t)] = \bar{a} N I^2 / 3$ is used. The asymptotic logarithmic decay agrees with the heuristic result of the introduction, and with the numerical findings of Ref. 10,13. Interestingly, the choice of k *does not* affect the prefactor of the leading logarithmic behavior in Eq.(71), suggesting that not only the logarithmic dependence but its prefactor might be properly obtained by this approach. The prefactor in (71) is indeed of the same order of magnitude as found in the $1/S^z - \ln t$ plot by Ref. 10, whose treatment is equivalent to a classical one with $I = S = \sqrt{3}/2$ in the equations of motion rather than $I = S = 1/2$.

We have carried out a similar calculation for an exponential wavefunction, $\gamma = 1$ in Eq.(6). In this case, we obtain

$$C(t) = \frac{4}{3} \frac{1}{\ln^2(t/k)}, \quad (72)$$

which is different from the asymptotic decay for the previous example, but agrees again with the arguments in the introduction. This disagrees with the suggestion in Ref.10 that the decay in this case would have the *same* form as for the Gaussian wavefunction above. However, no justification was given in Ref.10 for this claim apart from a slow growth of $1/\langle S^z(t) \rangle$ on a plot against $\ln t$. Given the spread in their numerical data, it is likely that the form of Eq.(72) would produce a good fit.

For the case of an infinitely high potential barrier in the quantum dot, the coupling constants vanishes at the boundary, and the electron only couples with a finite number of nuclear spin. The nuclear spins near the boundary have a coupling that vanishes quadratically with their distance from the boundary $g(r) \sim (1 - r/l)^2$, l being the radius of the confining barrier. Repeating the calculation above for this case, we find

$$C(t) \sim c_1 + c_2 \sqrt{\frac{k}{t}}, \quad (73)$$

where c_1 and c_2 are constants. This result can also be understood from the argument given in the Introduction. When $R(t)$ reaches the boundary of the confining potential, $R(t) = l(1 - \sqrt{k/t})$ and $N(t) = N(1 - \sqrt{k/t})^2$, where

N is the total number of nuclear spins. Plugging $N(t)$ into Eq.(5) leads to the above result.

VI. DISCUSSION

In this article we have derived the appropriate classical limit for the quantum central spin problem of a single electron spin coupled to many nuclear spins, and shown that this limit is indeed valid when the number of nuclei is large. This validates the starting point of Ref. 13, which simply assumed this. Furthermore, we have made some approximate analytic predictions for the asymptotic behavior of the central (electron) spin in this system, and have shown by numerical simulation that these predictions are roughly correct. Moreover, the approximations can be systematically improved, as we also described, though the technicalities involved in this improvement appear formidable. In the long-time limit for a finite number of nuclear spins, we argued that the asymptotic polarization of the electron spin will on average point in the direction of the total nuclear angular momentum \mathbf{I} , regardless of the coupling constants a_j . Finally, we have analytically derived the functional form of the decay of the electron spin polarization toward its asymptotic value. This form depends on the coupling constant profile, and is in qualitative and semi-quantitative agreement with observations from prior numerical investigations. Our results elucidates the physical origin of the long-time remanent spin polarization, and indicates that, remarkably, it is not connected to the integrability of the central spin problem.

The quite simple explanation of the long-time spin dynamics suggests that numerous extensions of these results should be possible, which are interesting in light of the relevance of the problem to experiments in quantum dots. Most obviously, one could likely explain the long-time behavior in situations with substantial nuclear polarization and/or applied magnetic fields, such as treated in some special cases in Refs.2,3. Our derivation of the classical limit in Sec.II was general enough to apply to these cases, so a treatment of this problem may proceed already from this point. Since integrability appears not to play a significant role, there also appears to be no substantial obstacle to analysis of more complex (and non-integrable) situations such as two electrons in near proximity coupled to overlapping nuclear populations, and crossover effects induced by weak nuclear dipole interactions. It would also obviously be interesting to treat more complicated dynamical quantities than the remanent electron spin described here, such as higher order spin autocorrelations, electron-nuclear entanglement, and the influence of time-dependent fields.

The more important and probably more formidable challenge is to connect the intriguing dynamical behavior of such electron-nuclear interaction problems to experiment. As was mentioned in the Introduction, the hyperfine interaction is the dominant source of dephas-

ing in current single-spin experiments in GaAs quantum dots. A recent review can be found in Ref.14. Existing experiments use optical^{15,16} or electrical^{17,18} means to measure this dephasing. These experiments, however, focus upon the short-time behavior, on the order of the electron precession frequency, in which the nuclear field can be regarded as approximately static. The non-trivial behavior which is the focus of this paper appears only on longer timescales. It is possible to use spin-echo techniques to remove the trivial dephasing effect of this fast electron precession about the (uncontrolled) quasi-static nuclear field^{19,20}. This technique (and possibly others) should in principle allow the unimpeded observation of the slower nuclear dynamics. Very recently, optical measurements have achieved the sensitivity necessary to measure a single electron spin in a *single* quantum dot.^{21,22} Direct observation of the electron spin in real time can of course also detect both short and long time dynamics. Given the sometimes frantic pace of experimental developments in this field, we hope that experimentalists as well as theorists will make the effort to explore some of this very interesting physics before rushing to more complex structures. It is conceivable that the confirmation of our physical picture of electron-nuclear spin interactions could even lead to useful ideas for future devices. For instance, the observation that the coupling profile determines the form of the electron spin polarization decay could enable control of time-dependent spin polarization by quantum dot shape engineering.

VII. ACKNOWLEDGMENT

We acknowledge discussions with V. Dobrovitski, and thank L. Glazman and D. Loss for stimulating our interest in the problem. This work was supported by the Packard Foundation and the National Science Foundation through grant DMR04-57440.

APPENDIX A: SELF-AVERAGING OF ELECTRON SPIN

In this appendix, we show that the fluctuations of the dynamics in initial conditions of the nuclear spin bath are negligible, thus demonstrating that the system is self-averaging. We will do so by proving Eq.(13).

We first consider $\hbar = 0$ in Eq.(10), in which case

$$\overline{\langle S^z(t) \rangle^2} = \sum_{\{m_i, m'_i, n_i, n'_i\}} \overline{C_{\{m_i\}}^* C_{\{n_i\}}^* C_{\{m'_i\}} C_{\{n'_i\}}} \\ \langle \{m_i\} | \langle \frac{1}{2} | S^z(t) | \frac{1}{2} \rangle | \{m'_i\} \rangle \langle \{n_i\} | \langle \frac{1}{2} | S^z(t) | \frac{1}{2} \rangle | \{n'_i\} \rangle, \quad (\text{A1})$$

where $Z = (2I + 1)^N$, and

$$\overline{C_{\{m_i\}}^* C_{\{n_i\}}^* C_{\{m'_i\}} C_{\{n'_i\}}} = \frac{\prod_i \delta_{m_i, m'_i} \delta_{n_i, n'_i} + \prod_i \delta_{m_i, n'_i} \delta_{m'_i, n_i}}{Z^2}, \quad (\text{A2})$$

With Eqs. (A1), (A2), we can express the variance of the spin expectation value, $\overline{\langle S^z(t) \rangle^2} - \overline{\langle S^z(t) \rangle}^2$ as

$$\frac{1}{Z^2} \sum_{\{m_i\}} \langle \{m_i\} | \langle \frac{1}{2} | S^z(t) | \frac{1}{2} \rangle \langle \frac{1}{2} | S^z(t) | \frac{1}{2} \rangle | \{m_i\} \rangle \quad (\text{A3})$$

In Eq.(A3), we have $\langle \frac{1}{2} | S^z(t) | \frac{1}{2} \rangle^2 \leq \frac{1}{4}$, resulting in a variance of

$$\overline{\langle S^z(t) \rangle^2} - \overline{\langle S^z(t) \rangle}^2 \leq \frac{1}{4Z^2} \sum_{\{m_i\}} \langle \{m_i\} | \{m_i\} \rangle = \frac{1}{4Z} \quad (\text{A4})$$

so the variance is of order $\sim Z^{-1} = (2I+1)^{-N}$. Since $\overline{\langle S^z(t) \rangle^2} \sim O(1)$, we find the $h \rightarrow 0$ limit of Eq.(13).

For the $h \neq 0$ case, an analogous derivation may be carried out, now including the Boltzmann-like factor $\tilde{\mathcal{H}} = -h \sum_i I_i^z$ as defined by Eq.(16). The variance now becomes

$$\begin{aligned} & \overline{\langle S^z(t) \rangle^2} - \overline{\langle S^z(t) \rangle}^2 \\ &= \frac{1}{Z^2} \sum_{\{m_i, n_i\}} |\langle \{m_i\}, \frac{1}{2} | S^z(t) | \frac{1}{2}, \{n_i\} \rangle|^2 e^{h \sum_i m_i + h \sum_i n_i} \\ &= \frac{1}{Z^2} \sum_{\{m_i\}} \langle \{m_i\} | e^{-\tilde{\mathcal{H}}} \langle \frac{1}{2} | S^z(t) | \frac{1}{2} \rangle e^{-\tilde{\mathcal{H}}} | \{m_i\} \rangle. \end{aligned} \quad (\text{A5})$$

Using $\langle \frac{1}{2} | S^z(t) | \frac{1}{2} \rangle \leq \frac{1}{2}$ we find a bound on the variance

$$\begin{aligned} & \overline{\langle S^z(t) \rangle^2} - \overline{\langle S^z(t) \rangle}^2 \\ & \leq \frac{1}{4Z^2} \sum_{\{m_i\}} \langle \{m_i\} | e^{-2\tilde{\mathcal{H}}} | \{m_i\} \rangle \\ &= \frac{1}{4Z^2} \left(\frac{\sinh((2I+1)h)}{\sinh(h)} \right)^N \quad (\text{A6}) \\ &= \frac{1}{4} \left(\frac{\tanh(\frac{h}{2})}{\tanh((I+\frac{1}{2})h)} \right)^N. \end{aligned}$$

With $\overline{\langle S^z(t) \rangle^2} \sim O(1)$, we have Eq.(13).

Since $\frac{\tanh(\frac{h}{2})}{\tanh((I+\frac{1}{2})h)} < 1$, in the large N limit, the above expression decays to zero exponentially.

APPENDIX B: APPROXIMATE DISTRIBUTION FUNCTION FOR THE EFFECTIVE NUCLEAR FIELD DIRECTION

In this appendix we find the distribution function for calculating (55), taking into account only the two most

significant conserved quantities.

$$\mathcal{Z}_1 = \int d\hat{\mathbf{m}} \int \mathcal{D}[\mathbf{I}_j] \delta(\mathbf{H}_N - \sum_i a_i \mathbf{I}_i) \delta(\mathbf{I} - \sum_i \mathbf{I}_i), \quad (\text{B1})$$

where $\hat{\mathbf{m}}$ is the directional vector of \mathbf{H}_N . First we use Lagrange multipliers to get the form

$$\mathcal{Z}_1 = \int d\hat{\mathbf{m}} \int d\mathbf{x} d\mathbf{y} e^{i\mathbf{x} \cdot \mathbf{H}_N + i\mathbf{y} \cdot \mathbf{I}} \int \mathcal{D}[\mathbf{I}_j] e^{-i \sum_i (\mathbf{x} \cdot a_i \mathbf{I}_i + \mathbf{y} \cdot \mathbf{I}_i)}. \quad (\text{B2})$$

Next we integrate over the \mathbf{I}_j variables

$$\mathcal{Z}_1 = \int d\hat{\mathbf{m}} \int d\mathbf{x} d\mathbf{y} e^{i\mathbf{x} \cdot \mathbf{H}_N + i\mathbf{y} \cdot \mathbf{I}} \prod_i \frac{\sin(I|a_i \mathbf{x} + \mathbf{y}|)}{I|a_i \mathbf{x} + \mathbf{y}|}, \quad (\text{B3})$$

where I is the magnitude of the nuclear spin vector. Now we use the thermodynamically large number of nuclear spins to first approximate the sum over nuclear spins by a distribution function $p(a)$ for the coupling constants, and then to justify a saddle point approximation

$$\begin{aligned} \prod_i \frac{\sin(I|a_i \mathbf{x} + \mathbf{y}|)}{I|a_i \mathbf{x} + \mathbf{y}|} &= e^{N \int da p(a) \ln \left(\frac{\sin(I|a\mathbf{x} + \mathbf{y}|)}{I|a\mathbf{x} + \mathbf{y}|} \right)} \\ &\approx e^{-\frac{NI^2}{6} \int da p(a) (a\mathbf{x} + \mathbf{y})^2} = e^{-\frac{NI^2}{6} (\bar{a}^2 \mathbf{x}^2 + 2\bar{a}\mathbf{x} \cdot \mathbf{y} + \mathbf{y}^2)}. \end{aligned} \quad (\text{B4})$$

Finally we integrate over the Lagrange multipliers \mathbf{x}, \mathbf{y} , and get

$$\mathcal{Z}_1 = \int d\hat{\mathbf{m}} e^{-\frac{3}{2} \frac{(H_N^2 + \bar{a}^2 I^2 - 2\bar{a}H_N I)}{NI^2(\bar{a}^2 - \pi^2)}}. \quad (\text{B5})$$

We define the probability distribution as follows

$$\mathcal{Z}_1 = \int d\cos(\theta) P_1(\cos \theta), \quad (\text{B6})$$

where θ is the angle between $\hat{\mathbf{m}}$ and $\hat{\mathbf{I}}$. The distribution function then takes the form

$$P_1(\cos \theta) = e^{\alpha \cos \theta}, \quad (\text{B7})$$

where $\alpha = \frac{3\bar{a}H_N I}{NI^2(\bar{a}^2 - \pi^2)}$ as defined in Sec. III D.

Similarly, simply introducing another Lagrange multiplier, we can find

$$P_2(\cos \theta) = e^{\gamma \cos \theta + \beta \cos^2 \theta}, \quad (\text{B8})$$

where β and γ are defined in Sec. III D.

For $P_p(\cos \theta)$ when $p > 2$, the calculation becomes more and more complicated, and hard to get an analytical expression.

¹ I. A. Merkulov, A. L. Efros, and M. Rosen, Phys. Rev. B **65**, 205309 (2002).

² A. V. Khaetskii, D. Loss, and L. Glazman, Phys. Rev. Lett.

- 88**, 186802 (2002).
- ³ A. Khaetskii, D. Loss, and L. Glazman, Phys. Rev. B **67**, 195329 (2003).
 - ⁴ W. X. Zhang, V. V. Dobrovitski, K. A. Al-Hassanieh, E. Dagotto, and B. N. Harmon, Phys. Rev. B **74**, 205313 (2006).
 - ⁵ K. A. Al-Hassanieh, V. V. Dobrovitski, E. Dagotto, and B. N. Harmon, Phys. Rev. Lett. **97**, 037204 (2006).
 - ⁶ S. I. Erlingsson and Y. V. Nazarov, Phys. Rev. B **70**, 205327 (2004).
 - ⁷ E. A. Yuzbashyan, B. L. Altshuler, V. B. Kuznetsov, and V. Z. Enolskii, journal of physics A-mathematical and general **38**, 7831 (2005).
 - ⁸ E. A. Yuzbashyan, V. B. Kuznetsov, and B. L. Altshuler, Phys. Rev. B **72**, 144524 (2005).
 - ⁹ A. Khaetskii, D. Loss, and L. Glazman, journal of superconductivity **16**, 221 (2003).
 - ¹⁰ K. A. Al-Hassanieh, V. V. Dobrovitski, E. Dagotto, and B. N. Harmon, Unpublished, cond-mat/0511681 (2005).
 - ¹¹ E. A. Yuzbashyan, B. L. Altshuler, V. B. Kuznetsov, and V. Z. Enolskii, J.Phys.A **38**, 7831 (2005).
 - ¹² A. Auerbach, *“Interacting Electrons and Quantum Magnetism”* (Springer-Verlag, New York, 1994).
 - ¹³ S. I. Erlingsson and Y. V. Nazarov, Phys. Rev. B **66**, 155327 (2002).
 - ¹⁴ R. Hanson, L. P. Kouwenhoven, J. R. Petta, S. Tarucha, and L. M. K. Vandersypen, Unpublished, cond-mat/0610433 (2006).
 - ¹⁵ P. F. Braun, X. Marie, L. Lombez, B. Urbaszek, T. Amand, P. Renucci, V. K. Kalevich, K. V. Kavokin, O. Krebs, P. Voisin, et al., Phys. Rev. Lett. **94**, 116601 (2005).
 - ¹⁶ M. V. G. Dutt, J. Cheng, B. Li, X. D. Xu, X. Q. Li, P. R. Berman, D. G. Steel, A. S. Bracker, D. Gammon, S. E. Economou, et al., Phys. Rev. Lett. **94**, 227403 (2005).
 - ¹⁷ A. C. Johnson, J. R. Petta, J. M. Taylor, A. Yacoby, M. D. Lukin, C. M. Marcus, M. P. Hanson, and A. C. Gossard, Nature **435**, 925 (2005).
 - ¹⁸ F. H. L. Koppens, J. A. Folk, J. M. Elzerman, R. Hanson, L. H. W. van Beveren, I. T. Vink, H. P. Tranitz, W. Wegscheider, L. P. Kouwenhoven, and L. M. K. Vandersypen, science **309**, 1346 (2005).
 - ¹⁹ J. R. Petta, A. C. Johnson, J. M. Taylor, E. A. Laird, A. Yacoby, M. D. Lukin, C. M. Marcus, M. P. Hanson, and A. C. Gossard, science **309**, 2180 (2005).
 - ²⁰ A. Greilich, D. R. Yakovlev, A. Shabaev, A. L. Efros, I. A. Yugova, R. Oulton, V. Stavarache, D. Reuter, A. Wieck, and M. Bayer, science **313**, 341 (2006).
 - ²¹ J. Berezovsky, M. H. Mikkelsen, O. Gywat, N. G. Stoltz, L. A. Coldren, and D. D. Awschalom, science **314**, 1916 (2006).
 - ²² M. Atature, J. Dreiser, A. Badolato, and A. Imamoglu, Nature Physics **3**, 101 (2007), ISSN 1745-2473.